Stark Spectroscopy of Excited-State Transitions in a Conjugated Polymer

C. Gadermaier,[1,2,*] F. Grasse,[3] S. Perissinotto,[1] M. Graf,[3] F. Galbrecht,[4] U. Scherf,[4] E. J. W. List,[3] and G. Lanzani[1]
[1]*National Laboratory of Ultrafast Science, Dipartimento di Fisica, Politecnico di Milano, P.zza L. da Vinci 32, 20133 Milano, Italy*
[2]*Department of Complex Matter, Jozef Stefan Institute, Jamova 39, 1000 Ljubljana, Slovenia*
[3]*Christian Doppler Laboratory Advanced Functional Materials, Institute of Solid State Physics, Graz University of Technology, A-8010 Graz, and Institute of Nanostructured Materials and Photonics, JOANNEUM RESEARCH A-8160 Weiz, Austria*
[4]*Department of Chemistry and Institute of Polymer Chemistry, Wuppertal University, Gauss-Str. 20, 42097 Wuppertal, Germany*
(Received 15 February 2007; published 4 February 2008)

Stark spectroscopy, which is well established for probing transitions between the ground and excited states of many material classes, is extended to transitions between transient *excited* states. To this end, it is combined with femtosecond pump-probe spectroscopy on a conjugated polymer with appropriately introduced traps which harvest excitation energy and build up a sufficient excited state population. The results indicate a significant difference in the effective dipole moments between two short lived excited states.

DOI: 10.1103/PhysRevLett.100.057401 PACS numbers: 78.66.Qn, 42.65.Re, 78.20.−e, 78.47.−p

Stark (electroabsorption, EA) spectroscopy has elucidated the electronic structure of many materials classes [1]. It reveals the changes of polarizability Δp and/or dipole moment Δm_f that accompany electronic transitions. Polarizability is a measure of electron delocalization, while a dipole moment indicates charge transfer. Yet, except in simple gas molecules, EA studies have been limited to transitions from the ground to an excited state. Given the importance of excited states in optoelectronics and nonlinear optics, we extend EA to transitions between transient *excited states*. This requires a high density of excited states and generation and probing of these states with fs time resolution.

To reach high densities of an excited state with a distinct spectral feature, we chose polyfluorene (PF), one of the best studied conjugated polymers [2,3], in which 5% of the fluorene units are replaced by fluorenone (FLO) [4–8]. FLO does not destroy the conjugation along the PF backbone and barely affects the primary excited singlet state S_1, but adds an excited state F_1 of lower energy [9]. Following photoexcitation in the FLO-free segments, energy is funneled to FLO-containing sites [10], which builds up substantial F_1 populations. We probe their EA via pump-probe spectroscopy with a modulated electric field. Besides the well-known field-induced S_1 dissociation [11–13], we find a clear EA signature of F_1, which is discussed in terms of an effective dipole moment.

In isotropic media, the change in the absorption coefficient α due to electric field F is

$$\Delta\alpha = \frac{1}{2}\Delta p F^2 \frac{\partial\alpha}{\partial E} + \frac{1}{6}(\Delta m_f F)^2 \frac{\partial^2\alpha}{\partial E^2} + c\alpha + \alpha' \qquad (1)$$

where E is energy and the last two terms describe transfer of oscillator strength from allowed ($c\alpha$, $c < 0$) to forbidden transitions (α').

In fs pump-probe spectroscopy, a pump pulse excites the sample and the relative change $\Delta T/T$ in optical transmission is measured with a probe pulse at a defined delay t. $\Delta T/T$ is proportional to the change ΔN_i in the population of states i, their effective absorption or emission cross sections σ_i, and the sample thickness d [14]:

$$\frac{\Delta T}{T}(E, t) = \sum_i \sigma_i(E)\Delta N_i(t)d. \qquad (2)$$

Field-induced changes in $\Delta T/T$ are

$$\begin{aligned}\frac{\Delta^2 T}{T} &= \sum_i \Delta(\sigma_i(E)\Delta N_i(t)d)\\ &= \sum_i \Delta\sigma_i(E)\Delta N_i(t)d + \sum_i \sigma_i(E)\Delta^2 N_i(t)d. \qquad (3)\end{aligned}$$

The first term describes changes in the cross sections due to Stark effect. The second term regards field-induced changes in the populations. The square differential accounts for the two perturbing factors: the pump beam and the electric field.

The chemical structure of the 95%/5% fluorene/fluorenone random copolymer (k-PF), is shown in Fig. 1. k-PF films of 100 nm thickness are sandwiched between Al and indium-tin oxide coated with poly(3,4-ethylenedioxythiophene) poly(styrenesulfonate). The fs pump-probe setup is described in [14]. An electric field modulated between 0 and 1.5×10^6 V cm^{-1} is applied in reverse bias to avoid charge injection.

The $\Delta T/T$ spectrum of k-PF is shown in Fig. 1 for different pump-probe delays. The positive signal above 2.4 eV is a combination of photobleaching (PB) due to depletion of S_0 and stimulated emission (SE) from S_1 [15,16]. The negative part (photoinduced absorption PA) changes with time, which indicates the contribution of at least two electronic states. The simplest model that correctly describes this behavior assumes three relaxation paths for S_1: directly to S_0, bimolecular recombination of two S_1, and migration to F_1:

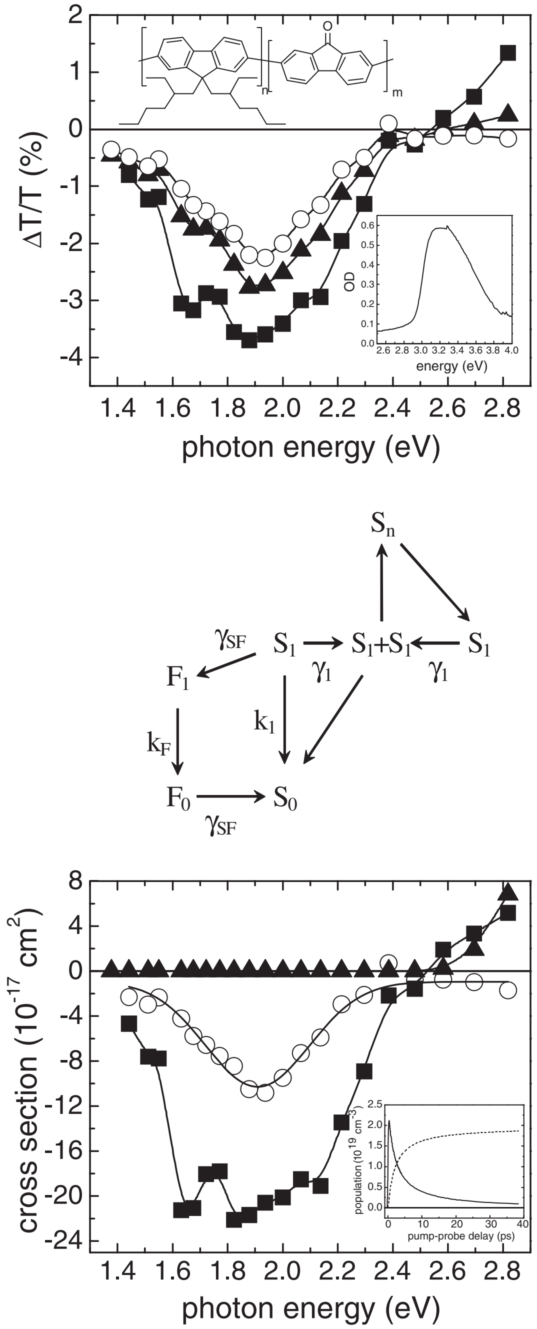

FIG. 1. Top: Pump-probe spectra of *k*-PF at 2 (squares), 8 (triangles), and 30 ps (open circles) pump-probe delay. Insets: chemical structure and absorption spectrum. Center: scheme of the assumed processes. Bottom: Absorption/emission cross sections of S_1 (squares), F_1 (open circles), and S_0 (triangles). S_1 and S_0 data points are connected with splines, F_1 data points with a Gaussian on a flat background. Inset: temporal evolution of S_1 (solid line) and F_1 (dash line) populations.

$$\begin{gathered} S_1 \longrightarrow S_0 \qquad S_1 + S_1 \longrightarrow S_n + S_0 \longrightarrow S_1 + S_0 \\ S_1 + F_0 \longrightarrow S_0 + F_1 \qquad F_1 \longrightarrow F_0 \end{gathered} \tag{4}$$

where S_0 and F_0 denote ground states of FLO-free and FLO-containing polymer segments. The temporal behavior of these populations can be described via rate equations:

$$\begin{gathered} \frac{dS_1}{dt} = G(t)S_0 - k_1 S_1 - \gamma_1 S_1^2 - \gamma_{SF} S_1 F_0 \\ \frac{dS_0}{dt} = -G(t)S_0 + k_1 S_1 + \gamma_1 S_1^2 + \gamma_{SF} S_1 F_0 \\ \frac{dF_1}{dt} = \gamma_{SF} S_1 F_0 - k_F F_1 \qquad \frac{dF_0}{dt} = -\gamma_{SF} S_1 F_0 + k_F F_1. \end{gathered} \tag{5}$$

$G(t)S_0$ is generation of S_1 via the laser pulse $\sim G(t)$ and the subsequent terms account for the processes described in Eqs. (4) in the same order of appearance, with rates k_i for monomolecular and rate parameters γ_i for bimolecular processes, respectively. To unravel the contributions of the various states, these equations have been used to fit time traces at four selected probe energies (1.51, 1.82, 2.14, and 2.82 eV). The temporal evolution of the S_1 and F_1 populations is shown as inset in Fig. 1. Knowing the S_0 absorption spectrum from transmission measurements and neglecting absorption from F_0 [7], the spectra of S_1 and F_1 can be extracted from the $\Delta T/T$ spectra using Eq. (2) (Fig. 1). The F_1 absorption is broad and featureless, like the absorption of PF, where the resolution of a vibronic structure is prevented by disorder and anharmonicity [17].

The field-modulated pump-probe spectrum $\Delta^2 T/T$ is depicted in Fig. 2. $\Delta^2 T/T$ and $\Delta T/T$ have opposite signs except at 2.0–2.5 eV. This is generally explained as dissociation of S_1 into polarons [11–13]. In Eq. (4), this would read

$$S_1 + S_0 \longrightarrow P^+ + P^-. \tag{6}$$

This process adds a time-dependent dissociation term $\gamma_d(t) S_1 S_0$ in Eqs. (5). P^+ and P^- are not distinguished in the spectrum, their joint population is called P. The complete rate equations with electric field thus read

$$\begin{gathered} \frac{dS_1}{dt} = G(t)S_0 - k_1 S_1 - \gamma_1 S_1^2 - \gamma_{SF} S_1 F_0 - \gamma_d(t) S_1 S_0 \\ \frac{dS_0}{dt} = -G(t)S_0 + k_1 S_1 + \gamma_1 S_1^2 + \gamma_{SF} S_1 F_0 - \gamma_d(t) S_1 S_0 \\ \frac{dF_1}{dt} = \gamma_{SF} S_1 F_0 - k_F F_1 \qquad \frac{dF_0}{dt} = -\gamma_{SF} S_1 F_0 + k_F F_1 \\ \frac{dP}{dt} = 2\gamma_d(t) S_1 S_0. \end{gathered} \tag{7}$$

The differences between the populations with and without field according to Eqs. (5) and (7) are the $\Delta^2 N_i$ in the second term of Eq. (3). With this model, we fit the $\Delta^2 T/T$ dynamics for the same wavelengths as above. The dissociation parameter $\gamma_d(t)$ decreases with a time constant of 1.3 ps, like for methyl-substituted poly(para-phenylene)-type ladder polymer (*m*-LPPP) at similar excitation densities [11].

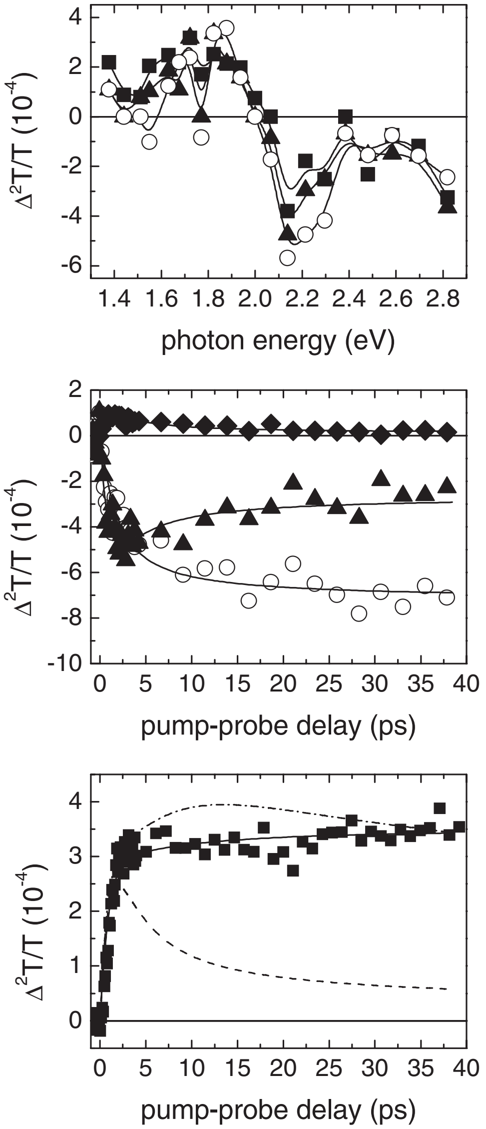

FIG. 2. Top: field-modulated pump-probe spectra at 2 (squares), 8 (triangles), and 30 ps (open circles) pump-probe delay. Center: field-modulated time traces at 1.51 (diamonds), 2.14 (open circles), and 2.82 eV (triangles). Full lines show fits of the dynamics. Bottom: time trace at 1.82 eV (squares). Fit according to Eqs. (5) and (7) (dashed line), including F_1 dissociation (dashed-dot line), including Stark effect of F_1 (solid line).

While the model using Eqs. (5) and (7) can very well fit three of the time traces (Fig. 2), it fails to reproduce the plateaulike shape at 1.82 eV. Thus, there is at least one additional effect of the electric field. Possible candidates are a change of one of the rate parameters k_1, γ_1, γ_{SF}, k_F, dissociation of F_1, additional dissociation or quenching of S_1 that does not result in polarons, or a contribution from the first term in Eq. (3): a Stark effect of either S_1 or F_1. By adding only one of these effects, the fit converges to negligible contributions for any of them except two: Stark effect of F_1 and dissociation of F_1. The latter leads to an unreasonable maximum around 15 ps (Fig. 2) and a bad fit of the other time traces (not shown), while a Stark contribution yields an excellent fit. The parameters used to obtain the best fit (i.e., with F_1 Stark effect) are listed in Table I.

Based on this fit, the F_1 Stark spectrum can be extracted via Eq. (3) from $\Delta^2 T/T$ like the S_1 and F_1 spectra from $\Delta T/T$ and is shown in Fig. 3, together with the first and second derivatives of the F_1 absorption. Transfer of oscillator strength to other transitions [last two terms in Eq. (1)] is negligible. The calculated Stark spectrum bears two main uncertainties, the noise of the measured $\Delta^2 T/T$ spectrum and the uncertainty of the fitted field-induced changes in the populations. Each of these independently contributes approximately 1×10^{-18} cm^2, so that the overall uncertainty is $\Delta\sigma_{\text{Stark}} = 1.4 \times 10^{-18}$ cm^2. Therefore, the fit in Fig. 3 has a reduced $\chi^2$of approximately $\chi_r \approx 1$, which confirms the validity of our model.

A first derivative line shape indicates a shift of the absorption, as would be the case for a difference in polarizability Δp between F_1 and F_n [Eq. (1)]. If different chromophores shift by different amounts, the width and height of the absorption peak (assuming a constant area, i.e., conservation of oscillator strength) change, which appears as a second derivative line shape, as is the case for our Stark spectrum. It is positive at the center, which means the absorption is lowered and broadened. To explain this via polarizability differences, one would need a balanced distribution of positive and negative Δp. This is possible but highly unlikely. A straightforward explanation is given by the second derivative term of Eq. (1), which originates from a difference in the effective dipole moments of F_1 and F_n. In isotropic samples, these are randomly oriented, and the scalar product $\Delta\vec{m}_f\vec{F}$ and hence the Stark shift is equally distributed between positive and negative values, which leads to the observed broadening of the absorption.

An effective dipole can arise either from a difference $\Delta\mu$ in ground and excited state permanent dipoles or from an effective internal field, which induces dipoles. This can have various origins. Strong local electric fields are caused by long lived polarons [18] from S_1 dissociation. Induced dipoles arise also from chemical defects like OH groups, which often appear at fluorenone units [19]. Stark effect from effective dipole moments has been observed on single molecules of both *m*-LPPP and phenylene vinylene (PPV)

TABLE I. C. Gadermaier *et al.*

$S_0(0)$ (cm^{-3})	1×10^{20}
$F_0(0)$ (cm^{-3})	2×10^{19}
k_1 (ps^{-1})	2.2×10^{-3}
γ_1 (cm^3 ps^{-1})	4.1×10^{-21}
γ_{SF} (cm^3 ps^{-1})	1.9×10^{-20}
γ_d (cm^3 ps^{-1})	$1.1 \times 10^{-22} \exp(t/1.4\text{ ps})$

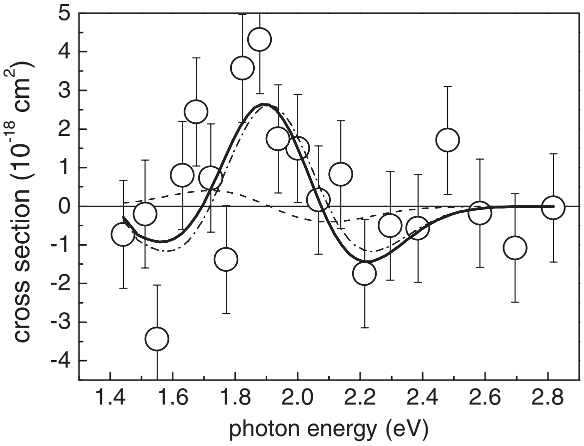

FIG. 3. F_1 Stark spectrum (open circles + error bars). Bold solid line shows fit to a sum of first (dashed line) and second (dashed-dot line) derivative of the F_1 absorption.

[20]. From the F_1 Stark spectrum, we estimate an effective $\Delta\mu$ between F_1 and F_n of 25 D, which is comparable to the 8 D observed for S_0-S_1 in PPV.

In summary, we have extended Stark spectroscopy to transitions between transient *excited states*. Our experiments quantify the difference in effective dipole moment between the involved excited states.

We highly appreciate the stimulating discussions with E. Zojer, M. Meneghetti, L. Lüer, M. Antognazza, and V. V. Kabanov. We acknowledge the support from LASERLAB-EUROPE, Contract Nos. RII3-CT-2003-506350, EUROFET-HPRN-CT-2002-00327, and POLITE-Fondazione CARIPLO. C. G. acknowledges the Erwin-Schrödinger Grant No. J2418-N02 from the Austrian Fonds zur Förderung der Wissenschaftlichen Forschung and the Marie-Curie Intra-European Fellowship No. 040958A. CDL-AFM acknowledges the continuous support from AT&S.

---

*Author to whom correspondence should be addressed: christoph.gadermaier@ijs.si

[1] G. Weiser and A. Horvath, in *Primary Photoexcitations in ConjugatedPolymers; Molecular Excitons vs. Semiconductor Band Model*, edited by N. S. Sariciftci (World Scientific, Singapore, 1997), and references therein.
[2] Y. Ohmori *et al.*, Jpn. J. Appl. Phys. **30**, L1941 (1991).
[3] A. W. Grice *et al.*, Appl. Phys. Lett. **73**, 629 (1998).
[4] E. J. W. List *et al.*, Adv. Mater. **14**, 374 (2002).
[5] J. M. Lupton, M. R. Craig, and E. W. Meijer, Appl. Phys. Lett. **80**, 4489 (2002).
[6] U. Scherf and E. J. W. List, Adv. Mater. **14**, 477 (2002).
[7] S. Gamerith *et al.*, Phys. Status Solidi A **201**, 1132 (2004).
[8] K. Becker *et al.*, Adv. Funct. Mater. **16**, 364 (2006).
[9] E. Zojer *et al.*, J. Chem. Phys. **117**, 6794 (2002).
[10] C. Gadermaier *et al.*, Phys. Rev. B **72**, 045208 (2005).
[11] W. Graupner *et al.*, Phys. Rev. Lett. **81**, 3259 (1998).
[12] V. Gulbinas *et al.*, Phys. Rev. Lett. **89**, 107401 (2002).
[13] T. Virgili *et al.*, Phys. Rev. Lett. **90**, 247402 (2003).
[14] T. Virgili *et al.*, in *Photophysics of Molecular Materials*, edited by G. Lanzani (Wiley-VCH, Weinheim, 2006).
[15] T. Virgili *et al.*, Appl. Phys. Lett. **74**, 2767 (1999).
[16] D. Kraabel *et al.*, Phys. Rev. B **61**, 8501 (2000).
[17] G. Heimel *et al.*, J. Chem. Phys. **122**, 054501 (2005).
[18] J. Orenstein, G. L. Baker, and Z. Vardeny, J. Phys. Colloq. **44**, C3-407 (1983).
[19] L. Romaner *et al.*, Chem. Mater. **16**, 4667 (2004).
[20] F. Schindler *et al.*, Nat. Mater. **5**, 141 (2006).